PAPER

Delay-Amplify-and-Forward Beamforming for Single-Carrier Relay Networks with Frequency Selective Channels

Hiroki TAKAHASHI[†*], ***Student Member and*** **Teruyuki MIYAJIMA**[††a)], ***Member***

SUMMARY In this paper, we propose a relaying strategy for single-carrier relay networks with frequency selective channels, where each relay node delays its received signal before amplify-and-forward processing it. We propose a computationally efficient delay design method which reduces the number of delay candidates. To further reduce computational complexity, we develop a simplified delay design method which reduces the number of weight computations. Also, we extend the design method to the case where only partial channel state information of relay-to-destination channels is available. Simulation results show that the proposed relaying strategy outperforms a conventional amplify-and-forward relaying strategy and achieves the performance close to that of a more complex filter-and-forward relaying strategy. It is also shown that the proposed delay design method achieves near-optimum performance.

key words: *amplify-and-forward, distributed beamforming, relay networks, inter-symbol interference, equalization*

1. Introduction

With the recent growth of mobile data services driven by the rapid spread of smartphones and tablets, there are increasing demands for high-speed wireless systems to enhance spectrum and power efficiency and improving network connectivity over a wide area. To meet such demands, relaying strategies have received much attention due to their attractive features such as low-cost deployment and low power consumption [1] and have been adopted in wireless standards such as IEEE WiMAX and 3GPP LTE-Advanced [2]. Among the various relaying strategies, amplify-and-forward (AF) [3] is the simplest scheme, where relay nodes only amplify the signal from the source and forward it to the destination.

If channel state information (CSI) is available at the relay nodes, relay beamforming (BF) with multiple relay nodes further enhances the system performance due to cooperative diversity [4]. There have been several studies on AF relay beamforming (AF-BF) [5]–[7]. These approaches have assumed that the source-to-relay and relay-to-destination channels are frequency flat. At relatively high data rate, however, the channels are frequency selective, and inter-symbol interference (ISI) is inevitable.

Manuscript received October 20, 2016.
Manuscript revised March 21, 2017.
Manuscript publicized May 19, 2017.

[†]The author is with the Graduate School of Science and Engineering, Ibaraki University, Hitachi-shi, 316-8511 Japan.
[††]The author is with the Department of Electrical and Electronic Engineering, Ibaraki University, Hitachi-shi, 316-8511 Japan.
[*]Presently, with Mobile Techno Corp.
a) E-mail: teruyuki.miyajima.spc@vc.ibaraki.ac.jp

DOI: 10.1587/transcom.2016EBP3391

The approaches to mitigate the ISI effect in relay networks fall into two categories. The first approach is to employ the orthogonal frequency division multiplexing (OFDM)-based AF relaying strategy [8], [9] where ISI can be removed by introducing a cyclic prefix (CP), which unfortunately reduces bandwidth efficiency. This strategy makes the relay nodes more complex because of the requirement of OFDM demodulation and remodulation at each relay node. Also, OFDM is not a good option if the system demands low peak-to-average power ratio (PAPR). In terms of low PAPR, single-carrier transmission techniques are preferable to OFDM. Block-based single-carrier transmission with frequency-domain equalization (SC-FDE) has been applied to AF relaying [10], [11]. Similar to OFDM-based AF relaying, however, the use of CP wastes bandwidth and each relay node requires complex operations. To the best of our knowledge, AF relaying strategies for continuous single-carrier relay networks with ISI have not been considered before. The second approach applies the filter-and-forward (FF)-BF technique to single-carrier transmission [12], [13]. In this approach, relay nodes utilize finite impulse response (FIR) filters to equalize the total channel from the source to the destination. In [12], the FIR filters are determined by maximizing the destination signal-to-interference-plus-noise ratio (SINR) subject to the total relay transmission power constraint. Also, the authors have shown that the filter design under the individual relay power constraints can be solved using convex optimization. The filter design requires the instantaneous CSI of all channels. In [13], an additional equalization at the destination is employed to improve the performance of FF-BF. The FF-BF strategies can reduce the ISI effect significantly at the expense of complicated processing at relay nodes.

In this paper, we propose a simple extension of the AF-BF strategy for continuous single-carrier relay transmission across frequency selective channels. In the proposed relaying strategy, each relay node delays its received signal before amplify-and-forward processing it. Unlike conventional AF-BF, by setting the individual delays properly, large gain paths in each channel can be combined to improve the performance with a slight increase of the complexity at relay nodes. We propose computationally efficient delay design methods. Moreover, we consider the case where the partial CSI of relay-to-destination channels is available as well as the case where the instantaneous CSI is available.

The rest of this paper is organized as follows. Section 2 describes the delay-amplify-and-forward relay network model. In Sect. 3, we propose the delay design methods using the full CSI, while in Sect. 4, the weight coefficients designs using the full CSI are explained. Section 5 provides the relay design using the partial CSI. In Sect. 6, simulation results are shown, followed by the conclusion in Sect. 7.

Throughout this paper, we use the following notations: $(\cdot)^T$, $(\cdot)^H$, and $(\cdot)^*$ represent the transpose, Hermitian transpose, and complex conjugate of a vector or matrix, respectively. $\mathrm{diag}\{\mathbf{a}\}$ denotes a diagonal matrix whose diagonal entries consist of the entries of vector $\mathbf{a}$. $\mathrm{tr}(\mathbf{A})$ represents the trace of $\mathbf{A}$. $\mathrm{vec}(\mathbf{A})$ forms a vector by stacking columns of $\mathbf{A}$. $\otimes$ denotes the Kronecher product. $\mathbf{I}_a$ represents the $a \times a$ identity matrix, $\mathbf{e}_i$ is the ith column on the identity matrix, and $\mathbf{0}_{a\times b}$ indicates the $a \times b$ zero matrix.

2. System Model

We propose a single-carrier relay network where relay nodes delay and amplify the received signals and then retransmit them to the destination, as shown in Fig. 1. We refer to it as *delay-amplify-and-forward* (DAF) relaying. The proposed relaying strategy is applicable in situations where AF has been used [2]. We assume that source-to-relay and relay-to-destination channels are frequency selective and that, similar to [6], [7], [12], no direct link between the source and the destination is available due to path loss or heavy shadowing.

We also assume that a central node, which is placed near relay nodes or is one of the relay nodes, has the full source-to-relay CSI and the full/partial relay-to-destination CSI. The central node collects all the CSI, which is estimated at each node using pilot symbols, and determines both the delays and the weight coefficients based on the CSI and then feeds them back to the relay nodes. The source-to-relay CSI is obtained by channel estimation at each relay node, and the relay-to-destination CSI is obtained by CSI feedback from the destination. Similar assumptions have been commonly made in the literature [12], [13].

The relay nodes operate in a half-duplex mode. Each transmission between the source node to the destination node consists of two phases. In the first phase, the source node with a single transmit antenna broadcasts its data packet to all the relay nodes. The data symbols s_k are taken from a signal constellation with variance P_s and are assumed to be independent, identically distributed (i.i.d.). The transmitted symbols are received by R relay nodes, each equipped with a single receive antenna. The received signal of the rth relay node at time k is given by

$$r_{r,k} = \sum_{n=0}^{L_f-1} f_{r,n}s_{k-n} + \eta_{r,k} = \mathbf{f}_r^T\hat{\mathbf{s}}_k + \eta_{r,k} \tag{1}$$

for $r = 1, \cdots, R$, where $f_{r,n}$ is the impulse response of the channel from the source to the rth relay node, whose length is L_f, $\eta_{r,k}$ is an additive white Gaussian noise (AWGN) with variance σ_η^2 at the rth relay node, $\mathbf{f}_r = \left[f_{r,0}, \cdots, f_{r,L_f-1}\right]^T$, and $\hat{\mathbf{s}}_k = \left[s_k, \cdots, s_{k-(L_f-1)}\right]^T$.

In the second phase, the relay nodes process the received signals and retransmit them. In the rth relay node, the received signal $r_{r,k}$ is delayed and amplified as

$$t_{r,k} = w_r^* r_{r,k-m_r} = w_r^*\mathbf{f}_r^T\hat{\mathbf{s}}_{k-m_r} + w_r^*\eta_{r,k-m_r} \tag{2}$$

where w_r and m_r represent the weight coefficient and the delay of the rth relay node, respectively. We assume that m_r takes a discrete value between $[0, D-1]$ where $D-1$ is the predetermined delay bound. Then, the rth relay node transmits the signal $t_{r,k}$ from a single transmit antenna.

The received signal at the destination node equipped with a single receive antenna at time k is given by

$$y_k = \sum_{r=1}^{R}\sum_{n=0}^{L_g-1} g_{r,n}t_{r,k-n} + \nu_k \tag{3}$$

where $g_{r,n}$ is the impulse response of the channel from the rth relay node to the destination, whose length is L_g, and ν_k is an AWGN with variance σ_ν^2 at the destination. The destination node detects the data symbol s_k from y_k using a simple slicer. Note that the destination does not require complicated processing or special expensive devices such as equalizers.

For later convenience, we rewrite the received signal in (3) using a vector notation. Substituting (2) to (3), we have

$$\begin{aligned} y_k &= \sum_{r=1}^{R} w_r^* \sum_{n=0}^{L_g-1} g_{r,n}\mathbf{f}_r^T\hat{\mathbf{s}}_{k-n-m_r} \\ &\qquad + \sum_{r=1}^{R} w_r^* \sum_{n=0}^{L_g-1} g_{r,n}\eta_{r,k-n-m_r} + \nu_k \\ &= \sum_{r=1}^{R} w_r^*\mathbf{g}_r^T\mathbf{F}_r\tilde{\mathbf{s}}_{k-m_r} + \sum_{r=1}^{R} w_r^*\mathbf{g}_r^T\boldsymbol{\eta}_{r,k-m_r} + \nu_k \\ &= \mathbf{w}^H\hat{\mathbf{G}}\mathbf{F}\mathbf{s}_k + \mathbf{w}^H\hat{\mathbf{G}}\boldsymbol{\eta}_k + \nu_k \end{aligned} \tag{4}$$

where

$$\mathbf{g}_r = \left[g_{r,0}, \cdots, g_{r,L_g-1}\right]^T,$$

$$\mathbf{F}_r = \begin{bmatrix} f_{r,0} & \cdots & f_{r,L_f-1} & 0 & \cdots & 0 \\ 0 & f_{r,0} & \cdots & f_{r,L_f-1} & \ddots & \vdots \\ \vdots & \ddots & \ddots & \ddots & \ddots & 0 \\ 0 & \cdots & 0 & f_{r,0} & \cdots & f_{r,L_f-1} \end{bmatrix} \in \mathbb{C}^{L_g\times(L_f+L_g-1)},$$

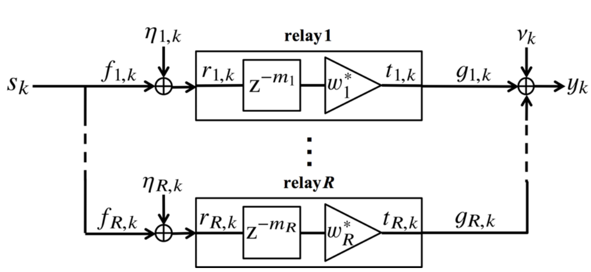

Fig. 1 Delay-amplify-and-forward relay network.

$$\tilde{\mathbf{s}}_{k-m_r} = \left[s_{k-m_r}, \cdots, s_{k-m_r-(L_f+L_g-2)}\right]^T,$$
$$\boldsymbol{\eta}_{r,k-m_r} = \left[\eta_{r,k-m_r}, \cdots, \eta_{r,k-m_r-(L_g-1)}\right]^T,$$
$$\mathbf{w} = [w_1, \cdots, w_R]^T,$$
$$\hat{\mathbf{G}} = \begin{bmatrix} \mathbf{g}_1^T & \mathbf{0}_{1\times L_g} & \cdots & \mathbf{0}_{1\times L_g} \\ \mathbf{0}_{1\times L_g} & \mathbf{g}_2^T & \ddots & \vdots \\ \vdots & \ddots & \ddots & \mathbf{0}_{1\times L_g} \\ \mathbf{0}_{1\times L_g} & \cdots & \mathbf{0}_{1\times L_g} & \mathbf{g}_R^T \end{bmatrix} \in \mathbb{C}^{R\times L_g R},$$
$$\mathbf{F} = \begin{bmatrix} \mathbf{0}_{L_g\times m_1} & \mathbf{F}_1 & \mathbf{0}_{L_g\times(m_{\max}-m_1)} \\ \vdots & \vdots & \vdots \\ \mathbf{0}_{L_g\times m_R} & \mathbf{F}_R & \mathbf{0}_{L_g\times(m_{\max}-m_R)} \end{bmatrix} \in \mathbb{C}^{L_g R\times(L_f+L_g-1+m_{\max})},$$
$$\mathbf{s}_k = \left[s_k, \cdots, s_{k-(L_f+L_g-2)-m_{\max}}\right]^T,$$
$$m_{\max} = \max\{m_1, \cdots, m_R\},$$
$$\boldsymbol{\eta}_k = \left[\boldsymbol{\eta}_{1,k-m_1}^T, \cdots, \boldsymbol{\eta}_{R,k-m_1}^T\right]^T.$$

Suppose that an element of $\mathbf{s}_k$, say $s_{k-\delta}$ where δ is a decision delay, is the desired symbol at time k, and thus the other elements correspond to ISI. More specifically, let $\bar{\mathbf{f}}_\delta$ denote the $(\delta+1)$th column of $\mathbf{F}$ and let $\bar{\mathbf{F}}_1$ and $\bar{\mathbf{F}}_2$ contain the remaining columns of $\mathbf{F}$ such that $\mathbf{F} = \left[\bar{\mathbf{F}}_1\ \bar{\mathbf{f}}_\delta\ \bar{\mathbf{F}}_2\right]$. Then, (4) can be rewritten as

$$\begin{aligned} y_k &= \mathbf{w}^H\hat{\mathbf{G}}\left[\ \bar{\mathbf{F}}_1\ \ \bar{\mathbf{f}}_\delta\ \ \bar{\mathbf{F}}_2\ \right]\begin{bmatrix} \bar{\mathbf{s}}_{\delta,1,k} \\ s_{k-\delta} \\ \bar{\mathbf{s}}_{\delta,2,k} \end{bmatrix} + \mathbf{w}^H\hat{\mathbf{G}}\boldsymbol{\eta}_k + \nu_k \\ &= \underbrace{\mathbf{w}^H\hat{\mathbf{G}}\bar{\mathbf{f}}_\delta s_{k-\delta}}_{y_{\mathrm{S},k}:\ \text{desired signal}} + \underbrace{\mathbf{w}^H\hat{\mathbf{G}}\bar{\mathbf{F}}\bar{\mathbf{s}}_{\delta,k}}_{y_{\mathrm{I},k}:\ \text{ISI}} + \underbrace{\mathbf{w}^H\hat{\mathbf{G}}\boldsymbol{\eta}_k + \nu_k}_{y_{\mathrm{N},k}:\ \text{noise}} \end{aligned} \quad (5)$$

where $\bar{\mathbf{F}} = \left[\bar{\mathbf{F}}_1\ \bar{\mathbf{F}}_2\right]$, $\bar{\mathbf{s}}_{\delta,k} = \left[\bar{\mathbf{s}}_{\delta,1,k}^T\ \bar{\mathbf{s}}_{\delta,2,k}^T\right]^T$, $\bar{\mathbf{s}}_{\delta,1,k} = [s_k, \cdots, s_{k-\delta+1}]^T$, $\bar{\mathbf{s}}_{\delta,2,k} = \left[s_{k-\delta-1}, \cdots, s_{k-(L_f+L_g-2)-m_{\max}}\right]^T$. In (5), there are three components corresponding to the desired signal, ISI, and noise components, respectively. We can intentionally change the total channel from the source to the destination by changing the delays $\{m_r\}$ as well as the weight coefficients $\{w_r\}$. Our goal is to maximize the destination SINR by properly determining both the delays and the weight coefficients:

$$\text{SINR} = \frac{E\left[|y_{\mathrm{S},k}|^2\right]}{E\left[|y_{\mathrm{I},k}|^2\right] + E\left[|y_{\mathrm{N},k}|^2\right]}. \quad (6)$$

3. Delay Design Using Full CSI

Let us consider the delay design when the instantaneous CSI of all channels $\{f_{r,k}, g_{r,k}\}$ is available. Before proceeding, we define a composite channel $h_{r,k}$ consisting of two physical channels $f_{r,k}$ and $g_{r,k}$ as

$$h_{r,k} = \sum_{n=0}^{L_f-1} f_{r,n}g_{r,k-n}, \quad k = 0, 1, \cdots, L_f + L_g - 2 \quad (7)$$

and form a vector $\mathbf{h}_r = \left[h_{r,0}, \cdots, h_{r,L_f+L_g-2}\right]^T$. Using the above notation, we obtain a composite channel matrix as

$$\mathbf{H} = \begin{bmatrix} \mathbf{0}_{1\times m_1} & \mathbf{h}_1^T & \mathbf{0}_{1\times(m_{\max}-m_1)} \\ \mathbf{0}_{1\times m_2} & \mathbf{h}_2^T & \mathbf{0}_{1\times(m_{\max}-m_2)} \\ \vdots & \vdots & \vdots \\ \mathbf{0}_{1\times m_R} & \mathbf{h}_R^T & \mathbf{0}_{1\times(m_{\max}-m_R)} \end{bmatrix} = \hat{\mathbf{G}}\mathbf{F} \in \mathbb{C}^{R\times(L_f+L_g-1+m_{\max})}. \quad (8)$$

The desired and ISI components can be represented as

$$\bar{\mathbf{h}}_\delta = \hat{\mathbf{G}}\bar{\mathbf{f}}_\delta, \quad (9)$$
$$\bar{\mathbf{H}} = [\bar{\mathbf{H}}_1\ \ \bar{\mathbf{H}}_2] = \hat{\mathbf{G}}\bar{\mathbf{F}}, \quad (10)$$

respectively, where $\bar{\mathbf{h}}_i$ is the $(i+1)$th column of $\mathbf{H}$, and $\bar{\mathbf{H}}_1$ and $\bar{\mathbf{H}}_2$ are the remaining columns of $\mathbf{H}$ such that $\mathbf{H} = [\bar{\mathbf{H}}_1\ \bar{\mathbf{h}}_\delta\ \bar{\mathbf{H}}_2]$.

3.1 Proposed Delay Design Method

Given the delay bound $(D-1)$, the total number of candidates of delays $\{m_1, \cdots, m_R\}$ is D^R. The larger D and R are, the better the performance we can expect. However, as D and R increase, the computational complexity to choose the best delays among the candidates becomes extremely high.

Now, we propose a computationally efficient method to determine the delays. The basic idea is to effectively reduce the number of delay candidates by focusing on only large gain paths in $\mathbf{h}_r$, and then choose one with the maximum SINR. The proposed procedure is summarized as follows:

Step1) Set $\delta \in [0, D-1]$ and $K \in [1, \min(L_f+L_g-1, \delta+1)]$. Find the K largest gain paths in each composite channel $h_{r,k}$ for $k = 0, \cdots, \delta$.

Step2) Determine K^R delay candidates such that the chosen paths are aligned at the predetermined time bin δ after delay processing.

Step3) For each candidate, solve the weight optimization problem described in Sect. 4.

Step4) Among the candidates, select the delays and weight coefficients, which provide the maximum SINR.

For easy understanding, we show an example of Steps 1 and 2 in Fig. 2 where each physical channel length is $L_f = L_g = 3$, the composite channel length is $L_f + L_g - 1 = 5$, the number of relays is $R = 3$, the number of chosen paths is $K = 2$ and $\delta = 4$.

- In Step1, we choose $K = 2$ largest paths in each channel; $\{h_{1,2}, h_{1,3}\}$, $\{h_{2,2}, h_{2,4}\}$ and $\{h_{3,3}, h_{3,4}\}$ in Fig. 2(a).
- In Step2, we set the delays. For the channel $h_{1,k}$, m_1 can be 2 or 1. If $m_1 = 2$, the largest gain path $h_{1,2}$ is placed on the time bin $\delta = 4$. If $m_1 = 1$, the second largest gain path $h_{1,3}$ is placed on the time bin.
- Similarly, m_2 can be 2 for $h_{2,2}$ or 0 for $h_{2,4}$; m_3 can be 1 for $h_{3,3}$ or 0 for $h_{3,4}$.
- Figure 2(b) shows the case of $(m_1, m_2, m_3) = (2, 0, 1)$, where $h_{1,2}$, $h_{2,4}$ and $h_{3,3}$ are aligned at the time bin

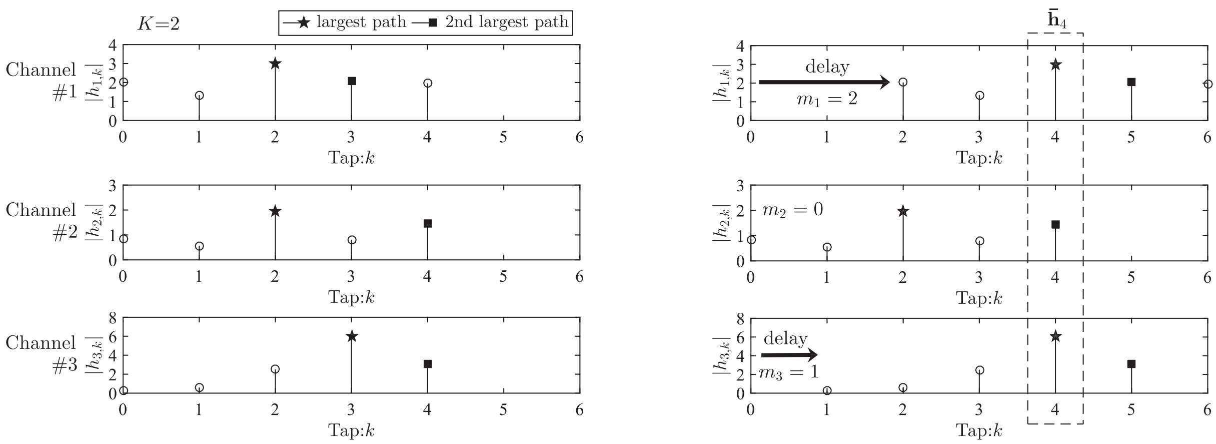

(a) Original channels before delay processing.

(b) Changed channels after delay processing.

Fig. 2 Example of Steps1 and 2 of the proposed delay design method. (a) Choose $K = 2$ largest gain paths in each original channel. (b) Align the chosen paths at the time bin $\delta = 4$ where delays are $(m_1, m_2, m_3) = (2, 0, 1)$. There are 7 other delay candidates since $K^R = 8$.

$\delta = 4$.

- There are 8 ($K^R = 2^3$) combinations of $(m_1, m_2, m_3) =$ (1, 0, 0), (1, 0, 1), (1, 2, 0), (1, 2, 1), (2, 0, 0), (2, 0, 1), (2, 2, 0), (2, 2, 1).

Let us discuss the choice of parameters, K, δ and D. As K increases, not only the performance improves but also the complexity increases. Thus, K should be chosen by taking into account both the required performance and the complexity. On the other hand, improved performance can be expected when the largest paths in each composite channel are aligned at the same time bin. To do so, δ should be at least the same as the length of composite channels, i.e., $\delta \geq L_f + L_g - 2$. Since demodulation delay should be as small as possible, we set $\delta = L_f + L_g - 2$. To obtain such δ, we should set $D - 1 \geq L_f + L_g - 2$. Since a large D is undesirable in terms of complexity, we set $D - 1 = L_f + L_g - 2$. Note that although these choices are not always the best, they serve as a useful guideline.

Note that the proposed method can reduce the number of delay candidates to K^R from D^R. The computational complexity of the proposed method is $C_1 + C_w \times K^R$ where $C_1 = O(L_f + L_g - 1) \times KR$ represents the computational complexity of the computation at Step1, and C_w represents the computational complexity required to solve the weight coefficients optimization problem as explained later.

3.2 Simplified Delay Design Method

At Step3 in the proposed delay design method, we require to solve the weight optimization problem K^R times. To further reduce computational complexity, we propose a simplified method whose idea is to evaluate the signal-to-interference ratio (SIR), which does not require the weight computation, rather than the SINR. After Steps 1 and 2 in Sect. 3.1, the following steps are performed:

Step3') For each candidate, evaluate SIR defined as

$$\mathrm{SIR} = \frac{\left\|\bar{\mathbf{h}}_\delta\right\|^2}{\sum_{i=0, i\neq\delta} \left|\bar{\mathbf{h}}_\delta^H \bar{\mathbf{h}}_i\right|}. \tag{11}$$

Step4') Among the candidates, select the delays that maximize SIR.

Step5') Using the delays, solve the weight optimization problem described in Sect. 4.

The SIR in (11) can be obtained by setting $\mathbf{w} = \bar{\mathbf{h}}_\delta$ in (5), i.e., maximum ratio combination (MRC). The delays obtained by the above procedure might provide suboptimal performance since MRC does not take into account ISI. Nevertheless, this method is computationally more efficient than the method in Sect. 3.1 because it requires the weight computation only once. Actually, the computational complexity of this method is $C_1 + C_2 + C_w$ where $C_2 = O(R) \times K^R$ represents the computational complexity of the computation at Step3'.

4. Weight Design Using Full CSI

As in the previous section, we assume that the instantaneous CSI of all channels $\{f_{r,k}, g_{r,k}\}$ is available. Before proceeding, we express the relay transmission powers and the destination SINR in terms of $\mathbf{w}$. From (1) and (2), the individual transmission power $E\left[\left|t_{r,k}\right|^2\right]$ of the rth relay node and the total transmission power of all relay nodes can be obtained as

$$p_r(\mathbf{w}) = w_r^* \left(P_s \mathbf{f}_r^T \mathbf{f}_r^* + \sigma_\eta^2\right) w_r = \mathbf{w}^H \mathbf{A}_r \mathbf{w}, \tag{12}$$

$$P(\mathbf{w}) = \sum_{r=1}^{R} p_r(\mathbf{w}) = \sum_{r=1}^{R} \mathbf{w}^H \mathbf{A}_r \mathbf{w} = \mathbf{w}^H \mathbf{A} \mathbf{w}, \tag{13}$$

respectively, where $\mathbf{A}_r = P_s \mathbf{E}_r \hat{\mathbf{F}} \hat{\mathbf{F}}^H \mathbf{E}_r^H + \sigma_\eta^2 \mathbf{E}_r \mathbf{E}_r^H$, $\mathbf{A} = \sum_{r=1}^{R} \mathbf{A}_r = P_s \hat{\mathbf{F}} \hat{\mathbf{F}}^H + \sigma_\eta^2 \mathbf{I}_R$, $\mathbf{E}_r = \mathrm{diag}\{\mathbf{e}_r\}$, and

$$\hat{\mathbf{F}} = \begin{bmatrix} \mathbf{f}_1^T & \mathbf{0}_{1\times L_f} & \cdots & \mathbf{0}_{1\times L_f} \\ \mathbf{0}_{1\times L_f} & \mathbf{f}_2^T & \ddots & \vdots \\ \vdots & \ddots & \ddots & \mathbf{0}_{1\times L_f} \\ \mathbf{0}_{1\times L_f} & \cdots & \mathbf{0}_{1\times L_f} & \mathbf{f}_R^T \end{bmatrix} \in \mathbb{C}^{R\times L_f R}.$$

Given delays m_r, the SINR in (6) is given by

$$\mathrm{SINR}(\mathbf{w}) = \frac{\mathbf{w}^H \mathbf{Q}_\mathrm{S} \mathbf{w}}{\mathbf{w}^H \mathbf{Q}_\mathrm{I} \mathbf{w} + \mathbf{w}^H \mathbf{Q}_\mathrm{N} \mathbf{w} + \sigma_\nu^2} \tag{14}$$

where $\mathbf{Q}_\mathrm{S}$, $\mathbf{Q}_\mathrm{I}$ and $\mathbf{Q}_\mathrm{N}$ are derived from (5) as

$$\mathbf{Q}_\mathrm{S} = P_s \hat{\mathbf{G}} \bar{\mathbf{f}}_\delta \bar{\mathbf{f}}_\delta^H \hat{\mathbf{G}}^H = P_s \bar{\mathbf{h}}_\delta \bar{\mathbf{h}}_\delta^H,$$
$$\mathbf{Q}_\mathrm{I} = P_s \hat{\mathbf{G}} \bar{\mathbf{F}} \bar{\mathbf{F}}^H \hat{\mathbf{G}}^H = P_s \bar{\mathbf{H}} \bar{\mathbf{H}}^H,$$
$$\mathbf{Q}_\mathrm{N} = \sigma_\eta^2 \hat{\mathbf{G}} \hat{\mathbf{G}}^H.$$

To determine weight coefficients w_r for given delays m_r, we use the common methods, which were applied to FF relaying in [12]. In the following, we briefly review the methods.

4.1 SINR Maximization Under Total Power Constraint

The first approach is to maximize the destination SINR subject to the constraint that the total relay transmission power P does not exceed its maximum relay transmission power budget P_max. This problem can be expressed as

$$\max_{\mathbf{w}} \ \mathrm{SINR}(\mathbf{w}) \ \text{ s.t. } \ P(\mathbf{w}) \le P_\mathrm{max}. \tag{15}$$

Using (13) and (14), we obtain the optimum weight coefficients vector and the maximum destination SINR as [12]

$$\mathbf{w}_\mathrm{opt} = \sqrt{P_\mathrm{max}} \mathbf{A}^{-1/2} \mathcal{P}\left\{\tilde{\mathbf{Q}}\right\}, \tag{16}$$
$$\mathrm{SINR}_\mathrm{max} = \mathcal{L}_\mathrm{max}\left\{\tilde{\mathbf{Q}}\right\}, \tag{17}$$

respectively, where $\mathcal{P}\{\cdot\}$ and $\mathcal{L}_\mathrm{max}\{\cdot\}$ denote the normalized principal eigenvector of a matrix and the largest eigenvalue of a matrix, respectively, and $\tilde{\mathbf{Q}} = \left(\tilde{\mathbf{Q}}_\mathrm{I+N} + \left(\sigma_\nu^2/P_\mathrm{max}\right)\mathbf{I}_R\right)^{-1}\tilde{\mathbf{Q}}_\mathrm{S}$, $\tilde{\mathbf{Q}}_\mathrm{S} = \mathbf{A}^{-1/2}\mathbf{Q}_\mathrm{S}\mathbf{A}^{-1/2}$, and $\tilde{\mathbf{Q}}_\mathrm{I+N} = \mathbf{A}^{-1/2}(\mathbf{Q}_\mathrm{I}+\mathbf{Q}_\mathrm{N})\mathbf{A}^{-1/2}$. The computational complexity required to solve (15) is dominated by the computation of eigenvalue decomposition. Therefore, the computational complexity is $C_w = O(R^3)$.

4.2 SINR Maximization Under Individual Power Constraints

In the second approach, we impose the constraints that the transmission power of each relay node p_r does not exceed its maximum relay transmission power budget $p_{r,\mathrm{max}}$. This is suitable for the case where the battery lifetime of each relay node is important. This problem can be expressed as

$$\max_{\mathbf{w}} \ \mathrm{SINR}(\mathbf{w}) \ \text{ s.t. } \ p_r(\mathbf{w}) \le p_{r,\mathrm{max}}, \ r = 1, \cdots, R, \tag{18}$$

and can be solved by the following bisection method [7]:

1) Set the initial interval $[\tau_l, \tau_u] = [0, \sqrt{\mathrm{SINR}_\mathrm{max}(P_\mathrm{max})}]$.

2) Set $\tau = (\tau_l + \tau_u)/2$.

3) Solve the following second-order cone programming (SOCP) problem:

$$\begin{aligned} &\text{find } \ \hat{\mathbf{w}} \\ &\text{s.t. } \ \sqrt{P_s}\hat{\mathbf{w}}^H\hat{\mathbf{h}} \ge \tau \|\mathbf{U}\hat{\mathbf{w}}\|, \\ &\qquad \|\mathbf{V}_r\hat{\mathbf{w}}\| \le \sqrt{p_{r,\mathrm{max}}}, \ \ r = 1, \cdots, R, \\ &\qquad \hat{\mathbf{w}}^H\mathbf{e}_1 = 1 \end{aligned} \tag{19}$$

where $\hat{\mathbf{w}} = \left[1, \mathbf{w}^T\right]^T$, $\hat{\mathbf{h}} = \left[0, \bar{\mathbf{h}}_\delta^T\right]^T$, $\hat{\mathbf{V}}_r = [\mathbf{0}_{R\times 1}, \mathbf{V}_r]$, $\mathbf{V}_r = \mathbf{A}_r^{1/2}$, and $\mathbf{U}$ is the Cholesky factorization of $\mathbf{B} = \begin{bmatrix} \sigma_\nu^2 & \mathbf{0}_{R\times 1}^T \\ \mathbf{0}_{R\times 1} & \mathbf{Q}_\mathrm{I} + \mathbf{Q}_\mathrm{N} \end{bmatrix}$. If it is feasible, $\tau_l = \tau$, otherwise $\tau_u = \tau$.

4) Repeat 2) and 3) until $(\tau_u - \tau_l) < \epsilon$.

$\mathrm{SINR}_\mathrm{max}(P_\mathrm{max})$ is obtained by (17) with $P_\mathrm{max} = \sum_{r=1}^R p_{r,\mathrm{max}}$. The allowed error tolerance value ϵ is set to a small value. Note that the problem (19) can be efficiently solved by using an SOCP solver such as SeDuMi [14] together with the modeling language YALMIP [15]. Its worst-case complexity is $C_w = O(R^{3.5})$.

Table 1 Computational complexity comparison.

	design phase: weight	design phase: delay	communication phase
DAF + MSINR	$O(R^3) \times K^R$	$O(L_f + L_g - 1) \times KR$	1
DAF + MSIR	$O(R^3)$	$O(L_f + L_g - 1) \times KR + O(R) \times K^R$	1
AF	$O(R^3)$	—	1
FF	$O(L_w^3 R^3)$	—	L_w

4.3 Complexity Analysis

The computational complexity of the various schemes is summarized in Table 1, where the total power constraint is assumed. "DAF + MSINR" and "DAF + MSIR" represent the proposed delay design method in Sect. 3.1 and the simplified method in Sect. 3.2, respectively. In the weight/delay design phase, the computational complexity of the DAF scheme can be higher than that of AF and FF. For small K, however, the computational increase of DAF is acceptable. Also note that this computation is performed not at relay nodes but at a central node, and is not required as long as the channels do not change. The computational complexity in the communication phase is more important since it is required at each relay node. As can be seen from the table, the DAF relay nodes require less computation than the FF relay nodes.

5. Relay Design Using Partial CSI

In Sects. 3 and 4, we assumed that the instantaneous CSI of all channels is available. It is not always easy to obtain the instantaneous CSI, especially for the relay-to-destination channels $\{g_{r,k}\}$ when the destination node is a mobile terminal. In this section, we consider the case where only partial

CSI of the relay-to-destination channels is available.

We employ the following model for the impulse response of the channel from the rth relay node to the destination [7]:

$$g_{r,n} = \sqrt{\frac{1}{1+\alpha}}\bar{g}_{r,n} + \sqrt{\frac{\alpha}{1+\alpha}}\tilde{g}_{r,n} \quad (20)$$

where $\bar{g}_{r,n}$ and $\tilde{g}_{r,n}$ are the mean and variable components of the complex path gain, respectively, and α is a parameter which determines the level of uncertainty. In the case of $\alpha = 0$, there is no variable component and it corresponds to the case of full CSI. As α increases, the deviation from the mean value becomes larger and the channel uncertainty becomes more severe. To prevent performance degradation in this case, we propose the delay and weight design methods based on the knowledge of the mean $\bar{g}_{r,n}$ and the second-order statistics (SOS) $E\left[g_{r,n}g^*_{r',n'}\right]$ of $g_{r,n}$.

5.1 Delay Design Using Partial CSI

To determine the delays, we propose to use the mean value $\bar{g}_{r,n}$ instead of the instantaneous value $g_{r,n}$. We consider the following composite channels:

$$\check{h}_{r,k} = \sum_{n=0}^{L_f-1} f_{r,n}\bar{g}_{r,k-n}. \quad (21)$$

Using the composite channels based on the mean $\bar{g}_{r,n}$, we can determine the delays by the methods in Sect. 3.

5.2 Weight Design Using Partial CSI

To derive the destination SINR, first, we calculate the desired signal power. The desired signal in (5) can be rewritten as $y_{\mathrm{S},k} = \mathbf{g}^T\bar{\mathbf{W}}^H\bar{\mathbf{f}}_\delta s_{k-\delta}$ where $\mathbf{g} = \left[\mathbf{g}_1^T, \cdots, \mathbf{g}_R^T\right]^T$, $\bar{\mathbf{W}} = \mathbf{W}\otimes\mathbf{I}_{L_g}$, and $\mathbf{W} = \mathrm{diag}\{\mathbf{w}\}$. Then, the desired signal power is given by†

$$\begin{aligned} E\left[|y_{\mathrm{S},k}|^2\right] &= P_s\bar{\mathbf{f}}_\delta^H\bar{\mathbf{W}}E\left[\mathbf{g}^*\mathbf{g}^T\right]\bar{\mathbf{W}}^H\bar{\mathbf{f}}_\delta \\ &= P_s\mathrm{tr}\left(\bar{\mathbf{W}}^H\bar{\mathbf{f}}_\delta\bar{\mathbf{f}}_\delta^H\bar{\mathbf{W}}\mathbf{\Phi}_\mathbf{g}^*\right) \\ &= P_s\left\{\mathrm{vec}\left(\bar{\mathbf{W}}^*\right)\right\}^T\left(\mathbf{\Phi}_\mathbf{g}^H\otimes\bar{\mathbf{f}}_\delta\bar{\mathbf{f}}_\delta^H\right)\mathrm{vec}\left(\bar{\mathbf{W}}\right) \\ &= P_s\mathbf{w}^H\mathbf{E}\left(\mathbf{\Phi}_\mathbf{g}^H\otimes\bar{\mathbf{f}}_\delta\bar{\mathbf{f}}_\delta^H\right)\mathbf{E}^H\mathbf{w} \\ &= \mathbf{w}^H\mathbf{Q}_{\mathrm{S,SOS}}\mathbf{w} \end{aligned} \quad (22)$$

where

$$\mathbf{Q}_{\mathrm{S,SOS}} = P_s\mathbf{E}\left(\mathbf{\Phi}_\mathbf{g}^H\otimes\bar{\mathbf{f}}_\delta\bar{\mathbf{f}}_\delta^H\right)\mathbf{E}^H,$$

$$\mathbf{\Phi}_\mathbf{g} = E\left[\mathbf{g}\mathbf{g}^H\right] = \frac{1}{1+\alpha}\left(\bar{\mathbf{g}}\bar{\mathbf{g}}^H + \alpha\mathbf{I}_{L_gR}\right),$$

$$\mathbf{E} = \left[\mathbf{E}_{1,1}\cdots\mathbf{E}_{1,L_g}\middle|\cdots\middle|\mathbf{E}_{R,1}\cdots\mathbf{E}_{R,L_g}\right] \in \mathbb{R}^{R\times L_g^2R^2},$$

$$\mathbf{E}_{r,l} = \left[\begin{array}{ccc}\mathbf{0}_{L_gR\times(r-1)} & \mathbf{e}_{(r-1)L_g+l} & \mathbf{0}_{L_gR\times(R-r)}\end{array}\right]^T \in \mathbb{R}^{R\times L_gR},$$

$\bar{\mathbf{g}} = \left[\bar{\mathbf{g}}_1^T, \cdots, \bar{\mathbf{g}}_R^T\right]^T$, and $\bar{\mathbf{g}}_r\left[\bar{g}_{r,0}, \cdots, \bar{g}_{r,L_g-1}\right]^T$. Similar to (22), the power of the ISI and noise components become

$$E\left[|y_{\mathrm{I},k}|^2\right] = \mathbf{w}^H\mathbf{Q}_{\mathrm{I,SOS}}\mathbf{w}, \quad (23)$$

$$E\left[|y_{\mathrm{N},k}|^2\right] = \mathbf{w}^H\mathbf{Q}_{\mathrm{N,SOS}}\mathbf{w} \quad (24)$$

where

$$\mathbf{Q}_{\mathrm{I,SOS}} = P_s\mathbf{E}\left(\mathbf{\Phi}_\mathbf{g}^H\otimes\bar{\mathbf{F}}\bar{\mathbf{F}}^H\right)\mathbf{E}^H,$$

$$\mathbf{Q}_{\mathrm{N,SOS}} = \sigma_\eta^2\mathbf{E}\left(\mathbf{\Phi}_\mathbf{g}^H\otimes\mathbf{I}_{L_gR}\right)\mathbf{E}^H.$$

We can apply the weight optimization problem (15) using (22)–(24).

†trace($\mathbf{ABCD}$) = $[\mathrm{vec}(\mathbf{A}^T)]^T(\mathbf{D}^T\otimes\mathbf{B})\mathrm{vec}(\mathbf{C})$ is used.

6. Simulation Results

Table 2 Simulation parameters.

Modulation scheme	QPSK
Maximum total relay power: $P_{\max}$	10 dB
Number of relays: R	7
Channel length: L_f, L_g	5
Delay bound: $D-1$	8
Decision delay: δ (AF, DAF)	(4, 8)

We conducted simulations to evaluate the performance of the DAF relaying strategy. Unless otherwise stated, the simulation parameters in Table 2 were used††. The noise powers were assumed to be $\sigma_\eta^2 = \sigma_\nu^2 = 1$; the source transmission power P_s was 10 dB higher than the noise power; and $P_{\max}$ in dB is relative to $\sigma_\eta^2 = \sigma_\nu^2$. The channel tap coefficients were modeled as $f_{r,k} \sim \mathcal{CN}(0,1)$, $g_{r,k} \sim \mathcal{CN}(0,1)$. The performances are evaluated by bit error rate (BER) rather than SINR, which is closely related to BER. BER was obtained by averaging over at least 100 simulation trials where each trial has different channels and different data.

First, we consider the case where the full CSI of all channels is available and the weight design method under the total relay power constraint in Sect. 4.1 is used.

Figure 3 demonstrates BER for various decision delay δ. As the composite channel length is $L_f+L_g-1 = 9$, δ can take between [0, 8]. For AF, $\delta = 4$ is the best because the middle path of composite channels is likely to be the largest gain path in the used channel model, while $\delta = L_f + L_g - 2 = 8$ for DAF provides the best performance as expected.

Figure 4 displays the effect of the number of chosen paths K on BER. Even if $K = 1$, the proposed methods outperform AF, and their performances improve as K increases.

In Fig. 5, the effect of the number of relays R on BER is shown. From this figure, we can see that BER improves by increasing R. Also, the required number of relays which

††$D-1$ and δ were set to the optimum values. R and K were chosen by considering the tradeoff between complexity and performance. For environment-dependent parameters P_s, $P_{\max}$, L_f and L_g, their values were just an example.

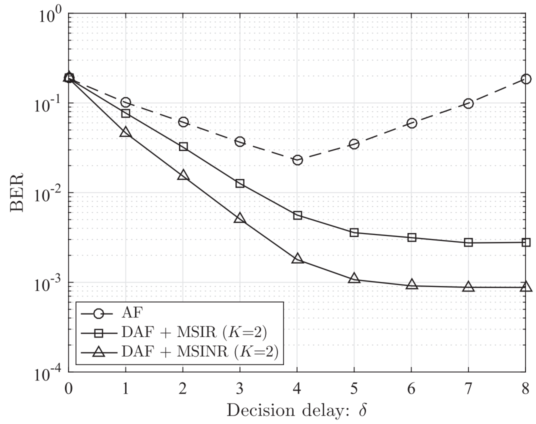

Fig. 3 Influence of decision delay δ on BER.

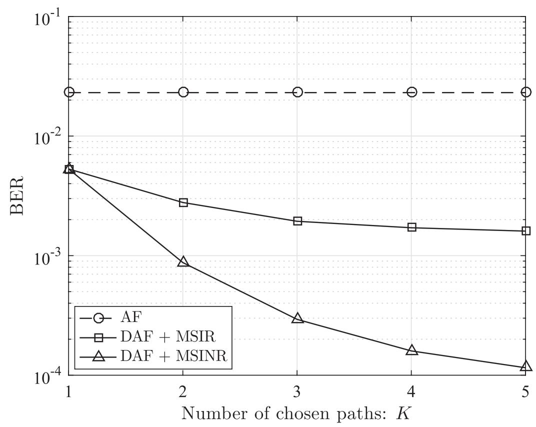

Fig. 4 Effect of the number of chosen paths K on BER.

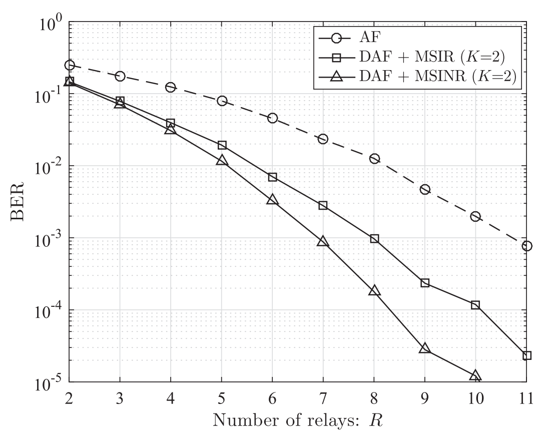

Fig. 5 Effect of the number of relays R on BER.

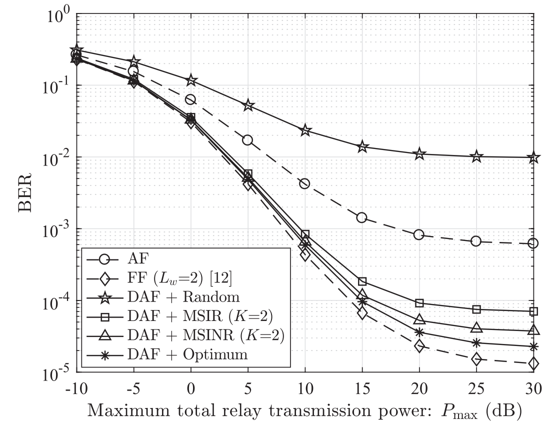

Fig. 6 BER versus maximum total relay transmission power $P_{\max}$.

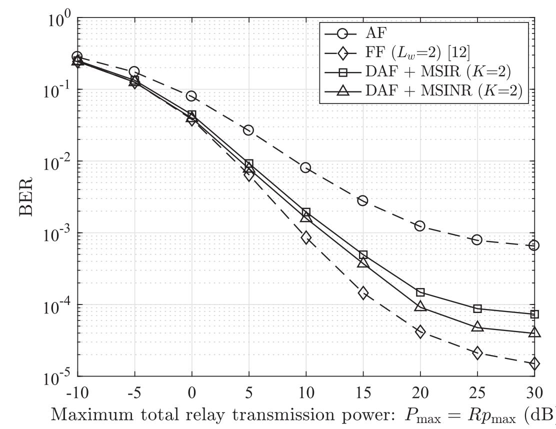

Fig. 7 BER in the case of individual relay power constraints.

achieves 10^{-3} of BER is 11 for AF, and 7 or 8 for DAF. This suggests that we can reduce the number of relays by DAF.

Figure 6 demonstrates BER for various maximum total relay transmission power $P_{\max}$, where $R = 5$, $L_f = L_g = 2$, $D - 1 = 4$, and $\delta(\mathrm{AF}, \mathrm{DAF}) = (1, 2)$. In this figure, "FF" represents the FF scheme using FIR filter of length L_w, "DAF + Optimum" represents the case where we solve (15) using the best delays among D^R possible combinations of the delays, and "DAF + Random" represents the case where each delay m_r is randomly set from $[0, D - 1]$. It can be seen that the DAF scheme is superior to AF and can achieve almost the same performance as FF with $L_w = 2$. Note that the complexity of the DAF relay nodes in the communication phase is half of that of the FF relay nodes. When the delays are set randomly, the performance is very poor. The performance of DAF using the proposed MSINR method achieves the performance by the optimum delays, and the performance of the proposed MSIR method is slightly inferior to that of the MSINR method.

Figure 7 shows the BER performances under the individual relay power constraints, where we used the same parameters as the previous example and $\epsilon = 10^{-3}$. In this simulation, we assumed that all the relay nodes have the same maximum transmission power budget, i.e., $p_{1,\max} = \cdots = p_{R,\max} = p_{\max}$, and $p_{\max} = P_{\max}/R$. Similar to Fig. 6, the DAF scheme outperforms AF and achieves the performance close to that of FF. However, the BER performances with the individual relay power constraints are a little inferior to those with the total relay power constraint because the individual power constraints are tighter than the total one.

Second, we consider the case where the partial CSI of the relay-to-destination channels is available. The mean

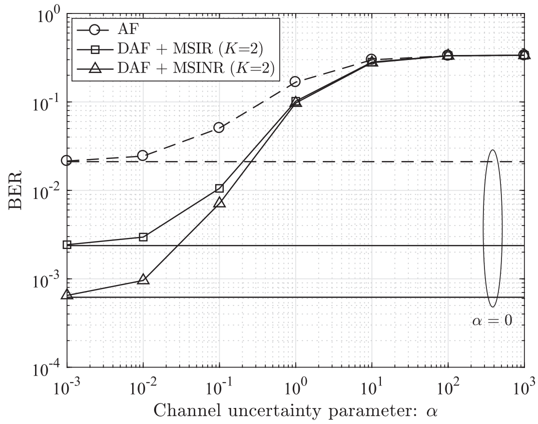

Fig. 8 Influence of uncertainty in the channel coefficients $g_{r,n}$

component $\bar{g}_{r,n}$ was generated according to $\mathcal{CN}(0,1)$ only once per simulation trial, and 100 realizations of the variable component $\hat{g}_{r,n}$ were generated according to $\mathcal{CN}(0,1)$ for each $\bar{g}_{r,n}$.

The BER performances for various α are shown in Fig. 8. As α increases, the channel uncertainty becomes severe and the performances degrade. Also, we can see that DAF with $\alpha = 10^{-1}$ outperforms AF with full CSI ($\alpha = 0$). Therefore, DAF is more robust to the channel uncertainty than AF.

7. Conclusion

In this paper, we proposed a delay-amplify-and-forward beamforming strategy for continuous single-carrier relay transmission across frequency selective channels. We also proposed computationally efficient delay design methods. Moreover, we considered the relay design using the partial CSI. It was shown that the proposed relaying strategy has better performance than the conventional AF relaying and achieves almost the same performance as a more complex FF relaying. Furthermore, the proposed delay design method achieved near-optimum performance.

References

[1] R. Pabst, B.H. Walke, D.C. Schultz, P. Herhold, H. Yanikomeroglu, S. Mukherjee, H. Viswanathan, M. Lott, W. Zirwas, M. Dohler, H. Aghvami, D.D. Falconer, and G.P. Fettweis, "Relay-based deployment concepts for wireless and mobile broadband radio," IEEE Commun. Mag., vol.42, no.9, pp.80–89, Sept. 2004.

[2] Y. Yang, H. Hu, J. Xu, and G. Mao, "Relay technologies for WiMax and LTE-advanced mobile systems," IEEE Commun. Mag., vol.47, no.10, pp.100–105, Oct. 2009.

[3] J.N. Laneman, D.N.C. Tse, and G.W. Wornell, "Cooperative diversity in wireless networks: Efficient protocols and outage behavior," IEEE Trans. Inf. Theory, vol.50, no.12, pp.3062–3080, Dec. 2004.

[4] A. Nosratinia, T.E. Hunter, and A. Hedayat, "Cooperative communication in wireless networks," IEEE Commun. Mag., vol.42, no.10, pp.74–80, Oct. 2004.

[5] Y. Jing and H. Jafarkhani, "Network beamforming using relays with perfect channel information," IEEE Trans. Inf. Theory, vol.55, no.6, pp.2499–2517, June 2009.

[6] G. Zheng, K.-K. Wong, A. Paulraj and B. Ottersten, "Collaborative-relay beamforming with perfect CSI: Optimum and distributed implementation," IEEE Signal Process. Lett., vol.16, no.4, pp.257–260, April 2009.

[7] V. Havary-Nassab, S. Shahbazpanahi, A. Grami, and Z.Q. Luo, "Distributed beamforming for relay networks based on second-order statistics of the channel state information," IEEE Trans. Signal Process., vol.56, no.9, pp.4306–4316, Sept. 2008.

[8] I. Hammerström and A. Wittneben, "Power allocation schemes for amplify-and-forward MIMO-OFDM relay links," IEEE Trans. Wireless Commun., vol.6, no.8, pp.2798–2802, Aug. 2007.

[9] H.A. Suraweera and J. Armstrong, "Performance of OFDM-based dual-hop amplify-and-forward relaying," IEEE Commun. Lett., vol.11, no.9, pp.726–728, Sept. 2007.

[10] P. Wu and R. Schober, "Cooperative beamforming for single-carrier frequency-domain equalization systems with multiple relays," IEEE Trans. Wireless Commun., vol.11, no.6, pp.2276–2286, June 2012.

[11] T.T. Pham, H.H. Nguyen, and H.D. Tuan, "Power allocation in MMSE relaying over frequency-selective Rayleigh fading channels," IEEE Trans. Commun., vol.58, no.11, pp.3330–3343, Nov. 2010.

[12] H. Chen, A.B. Gershman, and S. Shahbazpanahi, "Filter-and-forward distributed beamforming in relay networks with frequency selective fading," IEEE Trans. Signal Process., vol.58, no.3, pp.1251–1262, March 2010.

[13] Y. Liang, A. Ikhlef, W. Gerstacker, and R. Schober, "Cooperative filter-and-forward beamforming for frequency-selective channels with equalization," IEEE Trans. Wireless Commun., vol.10, no.1, pp.228–239, Jan. 2011.

[14] J.F. Sturm, "Using SeDuMi 1.02, a MATLAB toolbox for optimization over symmetric cones," Optimization Methods and Software, vol.11, no.1–4, pp.625–653, 1999.

[15] J. Löfberg, "YALMIP: A toolbox for modeling and optimization in MATLAB," Proc. 2004 IEEE International Symposium on Computer Aided Control Systems Design (CACSD), pp.284–289, Sept. 2004.

Hiroki Takahashi received the B.Eng. and M.Eng. degrees in electrical and electronic engineering from Ibaraki University, Hitachi, Japan, in 2015 and 2017, respectively. In 2017, he joined Mobile Techno Corp., Yokohama, Japan. His research interests include signal processing for wireless communications.

Teruyuki Miyajima received the B.Eng., M.Eng., and Ph.D. degrees in electrical engineering from Saitama University, Saitama, Japan, in 1989, 1991, and 1994, respectively. In 1994, he joined Ibaraki University, Hitachi, Japan, where he is currently a professor in the Department of Electrical and Electronic Engineering. His current interests are in signal processing for wireless communications. Dr. Miyajima is a member of IEEE.